

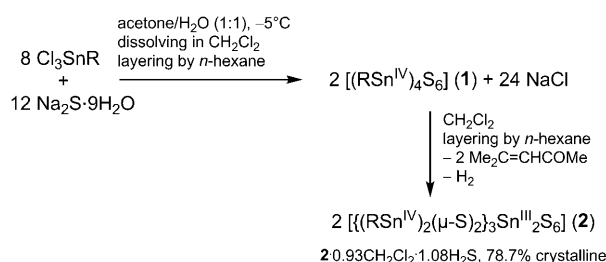
Thiostannate Tin–Tin Bond Formation in Solution: In Situ Generation of the Mixed-Valent, Functionalized Complex $[(\text{RSn}^{\text{IV}})_2(\mu\text{-S})_2]_3\text{Sn}^{\text{III}}_2\text{S}_6]^{\ast\ast}$

Zohreh Hassanzadeh Fard, Christian Müller, Thomas Harmening, Rainer Pöttgen, and Stefanie Dehnen*

In memory of Joachim Strähle

Tin–tin bonds are quite prevalent in inorganic^[1] and organo-element chemistry.^[2] Along with homo- or heteroatomic Zintl anions, recent derivatives with transition metal atoms, for instance $[\text{Pd}_2@\text{Sn}_{18}]^{4-}$ ^[3a] or $[(\eta^5\text{-C}_6\text{H}_5\text{Me})\text{Nb}]_2\text{Sn}_6]^{2-}$ ^[3b] have attracted attention because of their interesting dynamic behavior and uncommon bonding situations. Furthermore, reports on subvalent clusters, such as $[\text{Sn}_9\{\text{Sn}(\text{NR}'\text{R}'')\}_6]$ ($\text{R}' = \text{SiMe}_3$, $\text{R}'' = 2,6\text{-iPr}_2\text{C}_6\text{H}_3$),^[4] currently demonstrate a rich structural and electronic variety. Multifaceted organoelement compounds—dimers of different bond orders, charges, and ligands,^[2,5] chains,^[6] cycles,^[7] heterocycles,^[8,9] and polycycles^[7b,10]—serve to understand both analogies and differences to the carbon homologues, including the reactivity of the tin–tin bond. The synthesis and structural, magnetic, and electronic properties of compounds with further heteroatoms bonded to a tin–tin unit have been investigated, namely with boron^[11] or phosphorus atoms,^[12] such as $[(\text{SnB}_{10}\text{H}_{10})_2]^{2-}$,^[11a] $[(\text{SnB}_{10}\text{H}_{12})_2]^{2-}$,^[11b] or $[\text{Sn}(\mu\text{-PCy}_3)_3]^{2-}$.^[12b] Compounds with sulfur, selenium, and tellurium have also been investigated.^[13] The latter compounds are rare, especially with more than one or two chalcogen ligands; in particular, no compound containing a tin–tin bond and more than one sulfur ligand per tin atom has been reported to date. The prototypical $[\text{Sn}^{\text{III}}_2\text{E}_6]^{6-}$ anion is only known for $\text{E} = \text{Se}$ or Te .^[14]

Herein we present the in-situ transformation of a novel, double-decker thiostannate $[(\text{RSn})_4\text{S}_6]$ (**1**; $\text{R} = \text{CMe}_2\text{CH}_2\text{COMe}$) into the polynuclear complex $[(\text{RSn}^{\text{IV}})_2(\mu\text{-S})_2]_3\text{Sn}^{\text{III}}_2\text{S}_6 \cdot 0.93\text{CH}_2\text{Cl}_2 \cdot 1.08\text{H}_2\text{S}$ (**2**; $(\text{CH}_2\text{Cl}_2, \text{H}_2\text{S})$, Scheme 1). As confirmed by ^{119}Sn Mössbauer spectroscopy and quantum-chemical investigations, **2** is a mixed-valent complex that formally contains both tin(III) and tin(IV) atoms. Both compounds have $\text{C}=\text{O}$ functional groups; the



Scheme 1. Synthesis of compounds **1** and **2**; $\text{R} = \text{CMe}_2\text{CH}_2\text{COMe}$.

potential reactivity explains the motivation to study chalcogenidometallate complexes with organic ligands that are terminated by reactive units. The reaction of **1** to give hydrazones, such as $[(\text{H}_2\text{N}-\text{N}=\text{CMeCH}_2\text{CMe}_2\text{Sn})_4\text{S}_6]$, serves as a proof of principle.^[15] The complexes were structurally characterized by single-crystal X-ray diffraction,^[16] Figure 1 shows the molecular structures of both compounds. Details of the preparation of **1** and **2** and a full list of structural parameters is given in the Supporting Information.

The Sn/S core of **1** is not an adamantane-type cage, but adopts an isomeric, double-decker topology based on two parallel, $\mu\text{-S}$ -bridged Sn_2S_2 rings. Whereas this topology is well-known for silicon and germanium compounds,^[17a] it is rare in chalcogenidostannate chemistry.^[17b] Moreover, the ligands in **1** are involved in an intramolecular Lewis acid–base interaction via the keto group, with a coordination number (c.n.) of 5 at the tin atoms. ^{119}Sn NMR spectroscopic investigations of **1** in solution (Figure 2) confirm the predominance of the double-decker isomer ($\delta = 45.0, 95.5$ ppm) at room temperature, whereas the adamantane-type topology ($\delta = 97.9$ ppm) is formed upon heating in darkness. This observation is in accordance with DFT^[18,19] calculations of relative stabilities, which show an energetic preference of the double-decker Sn/S cage (**DD**) over the adamantane-type cage (**AD**) by about 20 kJ mol^{-1} . Additionally, the calculation of ^{119}Sn NMR shifts of all possible isomers with $N = 0\text{--}4$ open ligands, along with $4\text{--}N$ closed ligands (**DD**^{oN})^[20] indicate that **1** coexists in different conformers, most probably with 0, 1, or 2 open ligands (**DD**, **DD**^{o1}, **DD**^{o2}, Figure 2 f).

Isolated crystals of **1** do not show any reactivity under ambient conditions. However, if kept in the mother liquor under daylight, the compound undergoes a slow transformation into **2**: the mother liquor turns yellow, and yellow crystals of compound **2**, along with a yellow powder of the same

[*] Z. Hassanzadeh Fard, C. Müller, Prof. Dr. S. Dehnen
Fachbereich Chemie, Philipps-Universität Marburg
Hans-Meerwein-Strasse, Marburg (Germany)
Fax: (+49) 6421-282-5653
E-mail: dehnen@chemie.uni-marburg.de

T. Harmening, Prof. Dr. R. Pöttgen
Westfälische Wilhelms-Universität Münster
Corrensstrasse 30, 48149 Münster (Germany)

[**] This work was supported by the Deutsche Forschungsgemeinschaft, the Wissenschaftliches Zentrum für Materialwissenschaften, and the NRW Graduate School of Chemistry.

Supporting information for this article is available on the WWW under <http://dx.doi.org/10.1002/anie.200805719>.

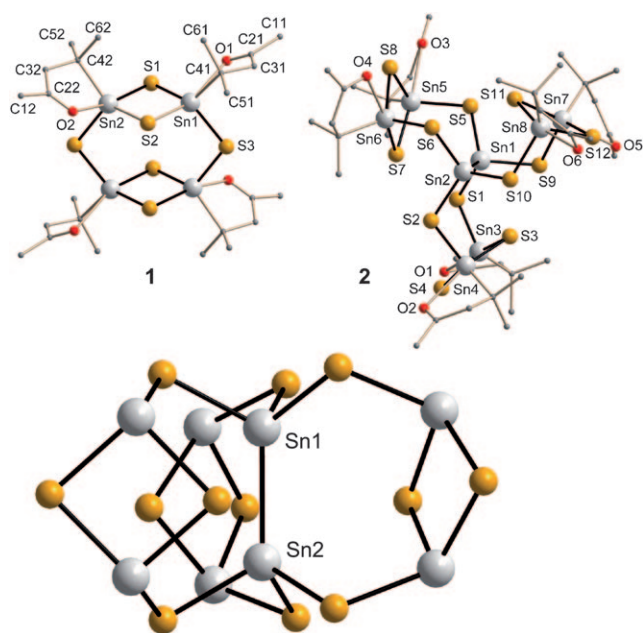


Figure 1. Molecular structures of **1** (top left) and **2** (top right: one of two crystallographically independent molecules; bottom: view of the Sn_8S_{12} skeleton). Hydrogen atoms and disordered carbon atoms are omitted for clarity. Selected bond lengths [pm]: **1**: Sn–S 238.92(15)–247.55(14), Sn–O 261.4(5)–267.2(4), Sn–C 217.9(5)–218.6(5). **2**: Sn–Sn 278.03(17)–280.39(17), Sn–S 239.7(5)–247.5(5), Sn–O 254.2(11)–272.9(25), Sn–C 213.2(16)–219.7(18).

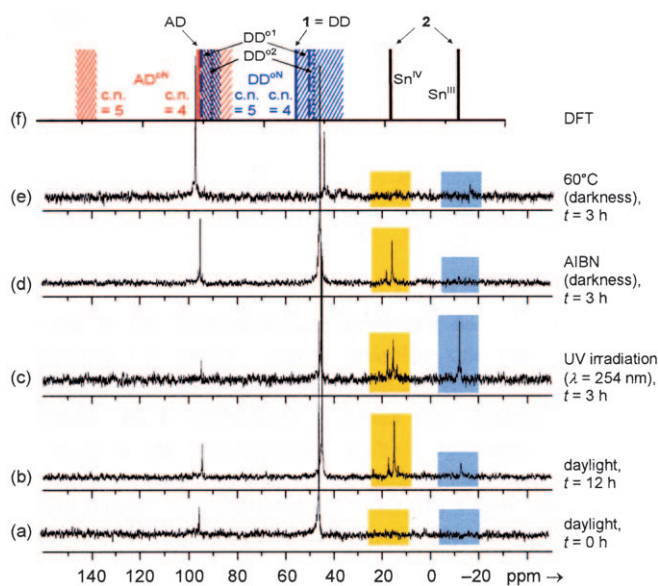


Figure 2. a–e) ^{119}Sn NMR spectra recorded during the reaction of **1** to form **2** under different conditions, and f) comparison with calculated chemical shift values for **1** and **2**. Signal ranges of double-decker fragments (yellow) and **2** (blue and yellow) are highlighted; spectrum (e) is shifted by 2 ppm to the right to make clear the peak height at 45 ppm. In (f), ranges are given for different double-decker or adamantane-type conformers DD^{0N} (red) or AD^{0N} (blue) with N open (c.n. = 4) and 4– N closed (c.n. = 5) ligands. Best agreements of calculated and experimental chemical shifts are indicated by bold lines.

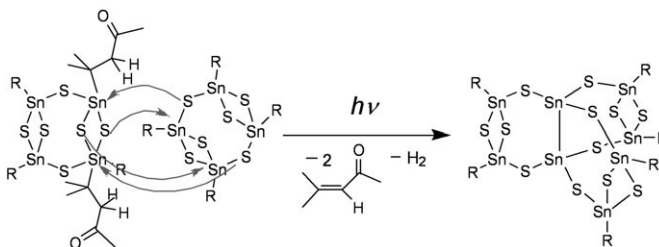
composition, appear within three days at the expense of the parent compound. After two weeks, compound **1** is no longer observed. Two signals upfield in the ^{119}Sn NMR spectrum that arise during the reaction ($\delta = -12.3$ ppm and around 15 ppm) can be assigned to the Sn^{III} and Sn^{IV} atoms of **2**, respectively.^[20]

The molecular structure of **2** has no precedence in chalcogenidostannate chemistry. A homoleptic, paddle-wheel-type arrangement of three $[(\text{R}\text{Sn})_2(\mu\text{-S})_2]\text{S}_2$ groups surrounds a central Sn1–Sn2 dumbbell with pseudo C_{3h} symmetry. The Sn–Sn bond length (Sn–Sn 278.03(17) pm, $\tilde{\nu}_{\text{Sn-Sn}}$ 174 cm^{-1}) is at the short end of the range of known values for Sn–Sn single bonds.^[1–15,21] The tin and sulfur atoms of the $[(\text{R}\text{Sn})_2(\mu\text{-S})_2]$ units in **2** form three four-membered rings at the end of the paddle wheels, which are part of three pairs of seven-membered rings that then share the Sn–Sn dumbbell.

Although the structure of **2** appears to be trimeric at first glance, with three fragments of **1** being attached to the tin–tin unit, a closer look at the two formulae clearly shows that **2** is a dimeric condensation product of **1**, with insertion of one of the double-decker rings into the other. The only difference between the composition of $2 \times \textbf{1}$ and of **2** is the loss of the two molecules R, which were identified as 4-methyl-3-penten-2-one (mesityl oxide) in the reaction mixture, plus one equivalent of H_2 . Time-dependent NMR spectra (Supporting Information, Figure S9) rationalize the generation of mesityl oxide during the reaction of **1** to **2**; the formation of H_2 was detected by absorption with palladium metal and subsequent reduction of molybdate(VI) by Pd/H_2 .^[22] The olefin is the oxidation product of the process, and two of the tin atoms in **2** (those forming the Sn–Sn dumbbell) are formally reduced to Sn^{III} , and two protons are reduced to H_2 by four electrons from two R molecules. Scheme 2 illustrates the condensation reaction.

As is typical for polynuclear chalcogenidometallate complexes, elucidation of the mechanism of formation is not trivial. To shed light on this point, we have performed further experimental and quantum chemical investigations. Besides the above-mentioned identification of the by-products, NMR spectroscopy studies were helpful in gaining insight in the ongoing processes. Figure 2 shows ^{119}Sn NMR spectra under different reaction conditions, together with calculated chemical shifts.

It can be seen from the NMR spectra (Figure 2 a–e) that compound **1** undergoes partial fragmentation in solution under light or radical initiation with (Figure 2 b, c) or without (Figure 2 d, e) formation of **2**. Thus, these fragments, which are



Scheme 2. Condensation reaction of **1** to form **2**: Rearrangement of Sn–S bonds and Sn–Sn bond formation are associated with Sn–C bond cleavage, producing mesityl oxide and H_2 . $\text{R} = \text{CMe}_2\text{CH}_2\text{COME}$.

presumably based on (RSn)₂S dimers or (RSn)₂S₂ four-membered rings similar to those reported for Ge/S analogues,^[23] are not essential to the formation mechanism of **2**. Their ¹¹⁹Sn NMR signals (δ = 13.9–17.5 ppm) are in the same range as the signal caused by the Sn^{IV}₂S₂ ring atoms in **2**, which complicates the differentiation. The upfield signal of **2** that arises under daylight, and is more pronounced upon UV irradiation, is however definitely hardly observed upon addition of AIBN or upon heating in darkness. This observation is in accordance with the observation that compound **2** does not crystallize from these samples; that is, it is neither formed in the dark, nor upon shifting the [(RSn)₄S₆] equilibrium toward the adamantane topology. The latter point is rationalized by the high structural relationship of **2** with **1** rather than with an adamantane cage.

The formation of a detectable intermediate containing Sn–H bonds from the leaving ligand R can be excluded, at least on the NMR timescale, as direct Sn–H coupling is never observed (³J = 130–200 Hz for all signals),^[24] which is in agreement with the ineffectiveness of radical initiation that might have provoked the generation of intermediate Sn–H bonds. Consequently, tin–tin bond formation from two L₃SnH precursors, which was reported for reactants with L = Me, Bu, Ph, F upon radical initiation by AIBN or irradiation,^[25a,26] can be ruled out. A comparison to calculated chemical shifts not only excludes the latter hypothesis, but also an intermediate with Sn–R groups instead of the Sn–Sn bond at the bridgehead atoms in **2**. We assume that the mechanism involves a light-induced transition state with a short lifetime and with weakened bonds—for instance upon suitable relative orientation of two double-decker molecules as indicated in Scheme 2—that undergoes rapid and concerted bond cleavage/bond formation. The high crystallization tendency of compound **2** acts as additional driving force toward the product. Based on this information, comprehensive theoretical studies are currently underway to model the transition state, including more complicated Sn/S cages and precursor aggregates.

DFT calculations reveal a reaction energy ΔE_R = 22.60 kJ mol^{−1} for the reaction according to Scheme 2, that is, being slightly endothermic in the gas phase. This situation is plausible if the bond balance is regarded: two four-coordinate tin atoms form, whereas two five-coordinate atoms were initially present, along with the different bond types of reactants versus products. To understand the observation of **2**, it is however necessary to assume a higher lattice energy of **2** than of **1** and to contemplate participation of the solvent.

To rationalize the different formal oxidation states in **2**, we measured ¹¹⁹Sn Mössbauer spectra of ground single crystals of **1** as a reference, and **2**. Figure 3 shows the spectra, and Table 1 summarizes the refined Mössbauer spectroscopic parameters.

Compound **1** produces a quadrupole-split signal at an isomer shift of 1.483(3) mm s^{−1} (Figure 3, left), in accordance with covalently bonded Sn^{IV} atoms (cf. the isomeric shift in SnS₂: 1.3 mm s^{−1}).^[27] Slight differences in the arrangement of the ligands around the tin atoms cause some line-broadening (that is, superposition of the signals of the two crystallographically independent tin atoms). The spectrum of **2**

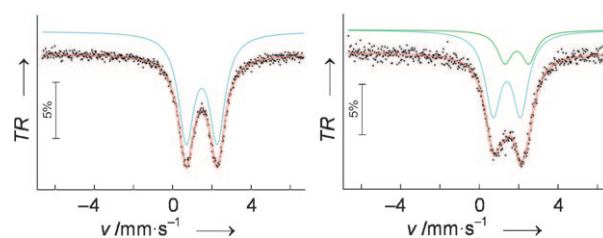


Figure 3. ¹¹⁹Sn Mössbauer spectra of **1** (left) and **2** (CH₂Cl₂, H₂S) (right) measured at 77 K. The red lines are fit curves for Sn^{IV} in **1** and Sn^{IV} (74%) and Sn^{III} (26%) in **2**. The subsets are marked in green and blue. TR = relative transmission.

Table 1: ¹¹⁹Sn Mössbauer spectroscopic investigation of ground single crystals of **1** and **2** at 77 K.^[a]

	δ	ΔE_Q	Γ	Formal oxidation state	I_R [%]
1	1.483(3)	1.58(4)	0.97(7)	+IV	100
2	1.39(7)	1.39(7)	0.97 ^[b]	+IV	74(1)
	1.9(1)	1.2(2)	0.9 ^[b]	+III	26(1)

[a] δ : isomer shift [mm s^{−1}], ΔE_Q : electric quadrupole splitting parameter [mm s^{−1}], Γ : experimental line width [mm s^{−1}], I_R : relative intensity. [b] Parameters held during the fitting procedure.

(Figure 3, right) can be well-modeled by two signals. One of them, with 74% intensity, is similar to that found in **1**, and is assigned to the twelve almost similar but crystallographically independent tin atoms of the two independent molecules with unchanged chemical environment. The second, with 26% intensity, shows an isomer shift (1.9 mm s^{−1}) right between the values typically observed for covalently bonded tin(II) atoms (3.4 mm s^{−1} for SnS)^[27] and covalently bonded tin(IV) atoms. Therefore, the four remaining tin atoms that form the two inner dumbbells of the two independent molecules are best described as being formally tin(III). This formulation is consistent with the ¹¹⁹Sn Mössbauer spectroscopic data obtained for [LFeSnFeL](PF₆)₂^[28] which contains a tin(III) species at an isomer shift of 2.00 mm s^{−1}. The strong quadrupole splitting of both signals of **2** results from the low site symmetries. These investigations are supported by natural population analyses (NPA)^[29] on the calculated complexes **1** and **2**: a natural charge of +1.36 is found at the formal tin(IV) atoms in both compounds, whereas the tin(III) atoms in the Sn–Sn dumbbell in **2** have only 76% of this natural charge value (+1.04).

In summary, the formation and stabilization of the unprecedented Sn^{III}₂S₆ unit is supported by reduction of the charge of the sulfur donor atoms by the attached Sn₂S₂ rings and adequate lattice energy of **2**. Future work includes the synthesis of related RT/E systems (T = Sn, Ge; E = S, Se, Te). Additionally, we are investigating reactions of **1** and **2** and its homologues with transition metal compounds, with nucleophiles targeting the Sn–Sn bond, and with organic molecules with complementary functionality to continue the journey toward multinary hybrid networks.

Received: November 24, 2008

Revised: December 22, 2008

Published online: March 12, 2009

Keywords: mixed-valent compounds · Mössbauer spectroscopy · thioestannates · tin–tin bonds · X-ray diffraction

- [1] a) J. D. Corbett, *Chem. Rev.* **1985**, 85, 383; b) T. Fässler, *Coord. Chem. Rev.* **2001**, 215, 347; c) R. Pöttgen, *Z. Naturforsch. B* **2006**, 61, 677.
- [2] a) P. P. Power, *Chem. Rev.* **1999**, 99, 3463; b) T. Tsumuraya, S. A. Batcheller, S. Masamune, *Angew. Chem.* **1991**, 103, 916; *Angew. Chem. Int. Ed. Engl.* **1991**, 30, 902; c) M. Weidenbruch, *J. Organomet. Chem.* **2002**, 646, 39.
- [3] a) Z.-M. Sun, H. Xiao, J. Li, L.-S. Wang, *J. Am. Chem. Soc.* **2007**, 129, 9560; b) B. Kesanli, J. Fetting, B. Eichhorn, *Angew. Chem.* **2001**, 113, 2364; *Angew. Chem. Int. Ed.* **2001**, 40, 2300.
- [4] M. Brynda, R. Herber, P. B. Hitchcock, M. F. Lappert, I. Nowik, P. P. Power, A. V. Protchenko, A. Ruzicka, J. Steiner, *Angew. Chem.* **2006**, 118, 4439; *Angew. Chem. Int. Ed.* **2006**, 45, 4333.
- [5] For recent examples see: a) R. Jambor, B. Kašná, K. N. Kirschner, M. Schürmann, K. Jurkschat, *Angew. Chem.* **2008**, 120, 1674; *Angew. Chem. Int. Ed.* **2008**, 47, 1650; b) E. Rivard, R. C. Fischer, R. Wolf, Y. Peng, W. A. Merrill, N. D. Schley, Z. Zhu, L. Pu, J. C. Fetting, S. J. Teat, I. Nowik, R. H. Herber, N. Takagi, S. Nagase, P. P. Power, *J. Am. Chem. Soc.* **2007**, 129, 16197; c) T. Fukawa, V. Ya. Lee, M. Nakamoto, A. Sekiguchi, *J. Am. Chem. Soc.* **2004**, 126, 11758.
- [6] a) K. Wiesler, N. Korber, *Z. Kristallogr.* **2005**, 220, 188; b) H. Puff, B. Breuer, G. Gehrke-Brinkmann, P. Kind, H. Reuter, W. Schuh, W. Wald, G. Weidenbrück, *J. Organomet. Chem.* **1989**, 363, 265; c) S. Adams, M. Dräger, *Angew. Chem.* **1987**, 99, 1280; *Angew. Chem. Int. Ed. Engl.* **1987**, 26, 1255.
- [7] a) S. P. Mallela, Y. Saar, S. Hill, R. A. Geanangel, *Inorg. Chem.* **1999**, 38, 2957; b) L. R. Sita, I. Kinoshita, *J. Am. Chem. Soc.* **1992**, 114, 7024; c) S. Masamune, L. R. Sita, *J. Am. Chem. Soc.* **1983**, 105, 630.
- [8] a) L. Baiget, H. Ranaivonjatovo, J. Escudie, H. Gornitzka, *J. Am. Chem. Soc.* **2004**, 126, 11792; b) C. Lee, J. Lee, S. W. Lee, S. O. Kang, J. Ko, *Inorg. Chem.* **2002**, 41, 3084; c) A. Krebs, A. Jacobsen-Bauer, E. Haupt, M. Veith, V. Huch, *Angew. Chem.* **1989**, 101, 640; *Angew. Chem. Int. Ed. Engl.* **1989**, 28, 603.
- [9] H. Grützmacher, H. Pritzkow, *Angew. Chem.* **1991**, 103, 976; *Angew. Chem. Int. Ed. Engl.* **1991**, 30, 1017.
- [10] a) N. Wiberg, H.-W. Lerner, H. Nöth, W. Ponikwar, *Angew. Chem.* **1999**, 111, 1176; *Angew. Chem. Int. Ed.* **1999**, 38, 1103; b) L. R. Sita, I. Kinoshita, *J. Am. Chem. Soc.* **1991**, 113, 1856.
- [11] a) D. Joosten, I. Pantenburg, L. Wesemann, *Angew. Chem.* **2006**, 118, 1103; *Angew. Chem. Int. Ed.* **2006**, 45, 1085; b) J. A. Dopke, D. R. Powell, R. K. Hayashi, D. F. Gaines, *Inorg. Chem.* **1998**, 37, 4160.
- [12] For recent examples, see: a) F. García, S. M. Humphrey, R. A. Kowenicki, E. J. L. McInnes, C. M. Pask, M. McPartlin, J. M. Rawson, M. L. Stead, A. D. Woods, D. S. Wright, *Angew. Chem.* **2005**, 117, 3522; *Angew. Chem. Int. Ed.* **2005**, 44, 3456; b) P. Alvarez-Bercedo, A. D. Bond, R. Haigh, A. D. Hopkins, G. T. Lawson, M. McPartlin, D. Moncrieff, M. E. G. Mosquera, J. M. Rawson, A. D. Woods, D. S. Wright, *Chem. Commun.* **2003**, 1288.
- [13] a) A. Schäfer, M. Weidenbruch, W. Saak, S. Pohl, H. Marsmann, *Angew. Chem.* **1991**, 103, 978; *Angew. Chem. Int. Ed. Engl.* **1991**, 30, 962; b) P. Brown, M. M. Mahon, K. C. Molloy, *J. Chem. Soc. Chem. Commun.* **1989**, 1621; c) H. Puff, B. Breuer, W. Schuh, R. Sievers, R. Zimmer, *J. Organomet. Chem.* **1987**, 332, 279; d) M. Dräger, B. Mathiasch, *Z. Anorg. Allg. Chem.* **1980**, 470, 45; e) H. Puff, B. Breuer, W. Schuh, R. Sievers, R. Zimmer, *J. Organomet. Chem.* **1983**, 248, 61.
- [14] a) B. Friede, M. Jansen, *Acta Crystallogr. Sect. C* **1999**, 55, 282; b) C. Zimmermann, S. Dehnen, *Z. Anorg. Allg. Chem.* **1999**, 453, 68; c) G. Dittmar, *Z. Anorg. Allg. Chem.* **1979**, 453, 68; d) S. Dehnen, M. Melullis, *Coord. Chem. Rev.* **2007**, 251, 1259; e) E. Ruzin, A. Kracke, S. Dehnen, *Z. Anorg. Allg. Chem.* **2006**, 632, 1018; f) S. Dehnen, C. Zimmermann, *Chem. Eur. J.* **2000**, 6, 2256.
- [15] Z. Hassanzadeh Fard, L. Xiong, C. Müller, M. Holyńska, S. Dehnen, unpublished results.
- [16] Crystal data: **1**: monoclinic, $P2_1/n$ (No 14), $a = 1166.6(5)$ pm, $b = 1270.1(4)$ pm, $c = 1235.9(5)$ pm, $\beta = 90.13(3)^\circ$, $V = 1831.2(12) \times 10^6$ pm³, $Z = 2$, $R(\text{int})$: 0.0889, final R ($I > 2\sigma(I)$), wR (all data): 0.040, 0.089; S (all data): 1.093. **2**: monoclinic, $P2_1/c$ (No. 14), $a = 2397.1(7)$ pm, $b = 2441.5(7)$ Å, $c = 2317.4(7)$ pm, $\beta = 90.56(3)^\circ$, $V = 13\,562(7) \times 10^6$ pm³, $Z = 8$, $R(\text{int})$: 0.0970, final R ($I > 2\sigma(I)$), wR (all data): 0.063, 0.190, S (all data): 0.999. Software used: G. M. Sheldrick, SHELXTL 5.1, Bruker AXS Inc., 6300 Enterprise Lane, Madison, WI 53719–1173, USA, **1997**. For more details of the X-ray crystal structure determination, see the Supporting Information. CCDC-709018 (**1**) and CCDC-709019 (**2**) contain the supplementary crystallographic data for this paper. These data can be obtained free of charge from The Cambridge Crystallographic Data Centre via www.ccdc.cam.ac.uk/data_request/cif.
- [17] a) M. Unno, Y. Kawai, H. Shioyama, H. Matsumoto, *Organometallics* **1997**, 16, 4428; b) R. A. Varga, C. Silvestru, *Acta Crystallogr. Sect. E* **2007**, 63, m2789.
- [18] a) R. G. Parr, W. Yang, *Density Functional Theory of Atoms and Molecules*, Oxford University Press, New York, **1988**; b) T. Ziegler, *Chem. Rev.* **1991**, 91, 651; accuracy of structural parameters $\Delta\delta = 1.4$ –11.4 pm for **1**, 0.8–13.1 pm for **2**.
- [19] Turbomole V5.10, Turbomole GmbH, Karlsruhe **2008**.
- [20] A systematic increment between observed and calculated chemical shifts is typical. Relative shift values are in good or excellent agreement with experiment: for example, $\Delta(\Delta\delta)_{\text{exp/calc}} = 4$ ppm for Sn^{IV} in **1**^{ol} versus **2**; $\Delta(\Delta\delta)_{\text{exp/calc}} = 1$ ppm for Sn^{IV} and Sn^{III} signals in **2**.
- [21] a) U. C. Rodewald, R.-D. Hoffmann, Z. Wu, R. Pöttgen, *Z. Naturforsch. B* **2006**, 61, 108; b) H. Schäfer, B. Eisenmann, W. Müller, *Angew. Chem.* **1973**, 85, 742; *Angew. Chem. Int. Ed. Engl.* **1973**, 12, 694.
- [22] C. Zhengelis, *Z. Anal. Chem.* **1911**, 49, 729. Experimental details are given in the Supporting Information.
- [23] H. Puff, K. Braun, S. Franken, T. R. Kök, W. Schuh, *J. Organomet. Chem.* **1987**, 335, 167.
- [24] B. Wrackmeyer in *Tin Chemistry—Fundamentals, Frontiers, and Applications* (Eds.: A. G. Davies, M. Gielen, K. H. Pannell, E. R. T. Tiekink), Wiley, Chichester, **2008**, p. 28.
- [25] a) C. Elschenbroich, *Organometallics*, 5th ed., Teubner, Wiesbaden, **2005**, p. 273; b) p. 174; c) p. 181.
- [26] a) A. G. Davies: *Organotin Chemistry*, 2nd ed., Wiley-VCH, Weinheim, **2004**, p. 249; b) B. Mathiasch in *Inorganic Reactions and Methods, Vol. 9/1* (Eds.: J. J. Zuckerman, A. P. Hagen), VCH, New York, **1991**, p. 77.
- [27] P. E. Lippens, *Phys. Rev. B* **1999**, 60, 4576; M. C. Hayes in *Chemical Applications of Mössbauer Spectroscopy* (Eds.: V. I. Goldanskii, R. H. Herber), Academic Press, New York, **1968**, p. 314; A. J. Boyle, D. S. P. Bunbury, C. Edwards, *Proc. Phys. Soc. London* **1962**, 79, 416.
- [28] T. Glaser, E. Bill, T. Weyhermüller, W. Meyer-Klaucke, K. Wieghardt, *Inorg. Chem.* **1999**, 38, 2632.
- [29] A. E. Reed, R. B. Weinstock, F. Weinhold, *J. Chem. Phys.* **1985**, 83, 735; note that natural charges do not represent formal oxidation states.